JACS
JOURNAL OF THE AMERICAN CHEMICAL SOCIETY
Communication
Cite This: J. Am. Chem. Soc. 2019, 141, 17995−17999
pubs.acs.org/JACS

Efficient Hydrogen Production from Methanol Using a Single-Site Pt_1/CeO_2 Catalyst

Lu-Ning Chen,[†,‡] Kai-Peng Hou,[†,§] Yi-Sheng Liu,[⊥] Zhi-Yuan Qi,[†] Qi Zheng,[†] Yi-Hsien Lu,[†] Jia-Yu Chen,[‡] Jeng-Lung Chen,[#] Chih-Wen Pao,[#] Shuo-Bo Wang,[†] Yao-Bin Li,[∇] Shao-Hua Xie,[○] Fu-Dong Liu,[○] David Prendergast,[∥] Leonard E. Klebanoff,[◆] Vitalie Stavila,[◆] Mark D. Allendorf,[◆] Jinghua Guo,[⊥] Lan-Sun Zheng,[‡] Ji Su,[*,†,∥] and Gabor A. Somorjai[*,†,§]

[†]Materials Sciences Division, [∥]Molecular Foundry, Material Science Division, and [⊥]Advanced Light Source, Lawrence Berkeley National Laboratory, Berkeley, California 94720, United States

[‡]State Key Laboratory of Physical Chemistry of Solid Surfaces, Collaborative Innovation Center of Chemistry for Energy Materials, and Department of Chemistry, College of Chemistry and Chemical Engineering, Xiamen University, Xiamen 361005, China

[§]Department of Chemistry, University of California—Berkeley, Berkeley, California 94720, United States

[#]National Synchrotron Radiation Research Center, Science-Based Industrial Park, Hsinchu 30076, Taiwan

[∇]Institute of Urban Environment, Chinese Academy of Sciences, Xiamen 361021, China

[○]Department of Civil, Environmental, and Construction Engineering, Catalysis Cluster for Renewable Energy and Chemical Transformations (REACT), Nano-Science Technology Center (NSTC), University of Central Florida, Orlando, Florida 32916, United States

[◆]Sandia National Laboratories, Livermore, California 94551, United States

Supporting Information

ABSTRACT: Hydrogen is regarded as an attractive alternative energy carrier due to its high gravimetric energy density and only water production upon combustion. However, due to its low volumetric energy density, there are still some challenges in practical hydrogen storage and transportation. In the past decade, using chemical bonds of liquid organic molecules as hydrogen carriers to generate hydrogen in situ provided a feasible method to potentially solve this problem. Research efforts on liquid organic hydrogen carriers (LOHCs) seek practical carrier systems and advanced catalytic materials that have the potential to reduce costs, increase reaction rate, and provide a more efficient catalytic hydrogen generation/storage process. In this work, we used methanol as a hydrogen carrier to release hydrogen in situ with the single-site Pt_1/CeO_2 catalyst. Moreover, in this reaction, compared with traditional nanoparticle catalysts, the single site catalyst displays excellent hydrogen generation efficiency, 40 times higher than 2.5 nm Pt/CeO_2 sample, and 800 times higher compared to 7.0 nm Pt/CeO_2 sample. This in-depth study highlights the benefits of single-site catalysts and paves the way for further rational design of highly efficient catalysts for sustainable energy storage applications.

In order to reduce atmospheric pollution and greenhouse gas emission, developing clean energy sources has attracted growing interest. Among them, hydrogen is desirable as an alternative clean fuel because it can be converted efficiently to energy without producing toxic products or greenhouse gases.[1] Nowadays, hydrogen is widely used in different fields, especially in polymer electrolyte membrane fuel cells (PEMFCs) due to its high gravimetric energy density (120 MJ/kg).[2] In contrast to other hydrogen transportation and storage approaches, such as compressed gas, or solid-state storage in metal hydrides or metal−organic frameworks (MOFs),[3,4] the liquid organic hydrogen carriers (LOHCs) concept involves transportation of hydrogen in liquids and generating hydrogen in situ by breaking chemical bonds, oftentimes in the presence of a catalyst.[5,6] There are advantages to transporting and handling liquids, such as added safety, greater energy density, and possibility of utilizing the existing gasoline and oil infrastructure and reduced costs overall.

For practical applications, a key factor is to look for an appropriate liquid organic molecule as hydrogen carrier.[7] Compared to other liquid organic molecules, methanol is a suitable molecule with high hydrogen gravimetric density. Moreover, methanol is relatively inexpensive and can be manufactured from a variety of sources, which can be transformed from some harmful gas or greenhouse gases like CO, CO_2, and CH_4.[8,9] In addition, seeking an efficient catalyst to in situ generate large quantity of hydrogen in a short time is another significant factor. In catalytic hydrogen production, the traditional support metal catalysts typically need high temperature and high metal loadings to achieve a relatively good catalytic performance.[10] As previously studied, the size of metal particles is critically important in determining the performance of metal-supported catalysts in many catalytic reactions.[11,12] Moreover, the ultimate small-size limit for particles is the

Received: September 4, 2019
Published: October 24, 2019

DOI: 10.1021/jacs.9b09431
J. Am. Chem. Soc. 2019, 141, 17995−17999

single-site catalyst with isolated single metal sites dispersed on solid supports. With maximum atom-utilization efficiency (100%), high specific activity and unique properties can be realized, single-site catalysts are emerging as a new frontier in catalytic science.[13−17]

Herein, we successfully synthesized single-site Pt_1/CeO_2 catalyst with single Pt sites anchored on porous CeO_2 supported by a modified ascorbic acid (AA)-assisted reduction route.[18,19] In the catalytic hydrogen production from methanol, compared with traditional Pt nanoparticle catalysts (2.5 nm Pt/CeO_2, 7.0 nm Pt/CeO_2), this single-site catalyst performed high activity at relatively low temperature with low Pt loading. Additionally, this single-site catalyst can be applied to other alcohol catalytic hydrogen production.

In our study, porous CeO_2 nanorods (Figure S1) were chosen as the support to anchor Pt single atoms by an AA-assisted reduction route, named Pt_1/CeO_2. Meanwhile, we also synthesized Pt nanoparticles with different sizes and loaded on CeO_2 by presynthesizing Pt nanoparticles and mixing them with CeO_2, and the capping agent on Pt surface was further removed by UV-ozone treatment.[20,21] The loading amounts of Pt both were about 1% wt. For convenience, the Pt nanoparticles loaded on CeO_2 are named 2.5 nm Pt/CeO_2 and 7.0 nm Pt/CeO_2, whose sizes are determined by TEM measurement (Figure S2).

The loading status of Pt loading on CeO_2 catalysts were compared by powder X-ray diffraction (XRD) and transmission electron microscope (TEM). From the XRD data, there are no diffraction peaks observable from metallic Pt for all the three catalysts due to the low Pt content and small Pt particle sizes (Figure S3). In the bright-field TEM images of 2.5 nm Pt/CeO_2 and 7.0 nm Pt/CeO_2, Pt nanoparticles are uniformly dispersed on CeO_2 nanorods (Figure S4b,c). However, for Pt_1/CeO_2 catalyst there is no apparent difference compared to original CeO_2 nanorods (Figure S1a), with no metallic clusters or particles being observed (Figure S4a). Moreover, from corresponding elemental mapping, the Pt signals are uniformly distributed over all CeO_2 nanorods (Figure 1b). In order to further confirm the actual Pt loading

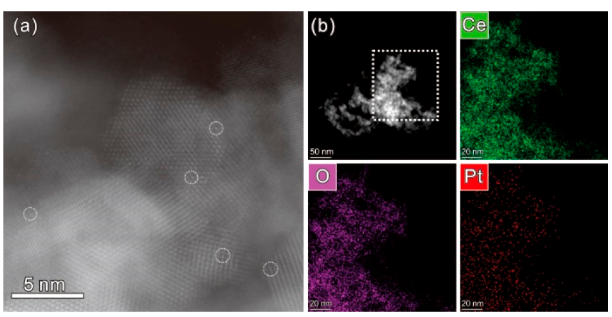

Figure 1. (a) Cs-corrected high-angle annular dark-field scanning transmission electron microscopy (HAADF-STEM) images of Pt_1/CeO_2 catalyst, the brighter circled dots are Pt single sites. (b) HAADF-STEM and corresponding elemental mapping images of Pt_1/CeO_2 catalyst.

information on CeO_2, the HAADF-STEM measurement was applied. As shown in Figure 1a, the Pt catalytic sites were atomically dispersed throughout the porous CeO_2, and the actual Pt content was 0.15%.

Extended X-ray absorption fine structure (EXAFS) spectra were acquired to provide the valence and coordinated structure of a single-site Pt_1/CeO_2 catalyst. Compared with bulk Pt foil there is no nearest neighbor Pt−Pt bond observed in the single-site Pt_1/CeO_2 catalyst, while the notable peak observed between 1 to 2 Å is attributed to contribution of the Pt−O bond (Figure 2). The Pt dispersion states for the three samples

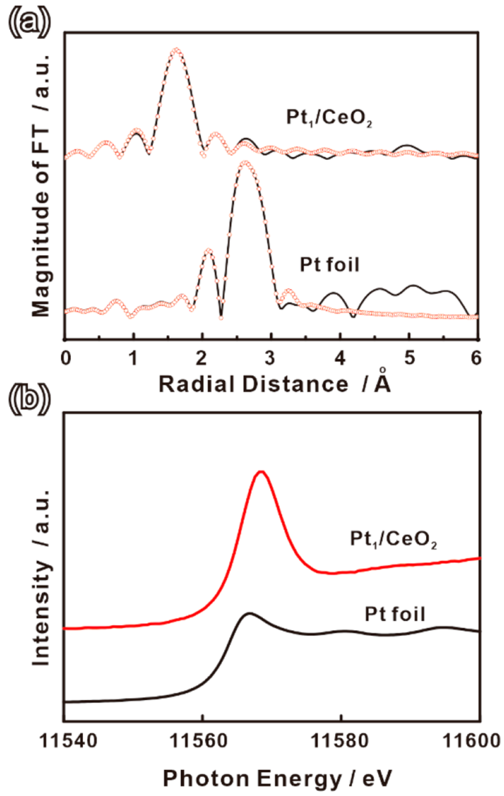

Figure 2. (a) k^3-weighted Fourier-transform EXAFS spectra and (b) normalized XANES spectra of Pt_1/CeO_2 and bulk Pt foil at the Pt L_3-edge. The red hollow points are fitting results.

are further verified by in situ DRIFTs of CO absorption and desorption (Figure S5). For the single-site Pt_1/CeO_2 catalyst, three bands are observed, of which the bands at 2171 and 2117 cm^{-1} are attributed to the CO gas, while that at 2090 cm^{-1} are attributed to the linearly (on-top) bonded CO on Pt ionic species.[13,18] However, for 2.5 nm Pt/CeO_2 and 7.0 nm Pt/CeO_2, there is another band at 2050 cm^{-1} due to the linear absorbance of CO on the small sized Pt nanoparticles on CeO_2.[13,22]

In the direct methanol catalytic hydrogen production, compared with traditional Pt nanoparticles (2.5 nm Pt/CeO_2 and 7.0 nm Pt/CeO_2), the single-site Pt loaded on CeO_2 (Pt_1/CeO_2) displayed excellent catalytic performance (Figure 3a). At the temperature below 150 °C, both the Pt single-site and Pt nanoparticle catalysts have no obviously catalytic activity. As the temperature was increased to above 150 °C, both the formation of hydrogen and carbon monoxide were detected. Further increasing the reaction temperature, more methanol was converted to hydrogen and carbon monoxide. Moreover, due to the size effect, the single-site Pt_1/CeO_2 catalyst performed with higher activity for hydrogen production from methanol than the 7.0 nm Pt/CeO_2 and 2.5 nm Pt/CeO_2 counterparts. The turnover frequency (TOF) of Pt_1/CeO_2 catalyst is much higher than traditional Pt nanoparticle, up to 12 500 h^{-1} at 300 °C, which is 40 times that of 2.5 nm Pt/

DOI: 10.1021/jacs.9b09431
J. Am. Chem. Soc. 2019, 141, 17995−17999

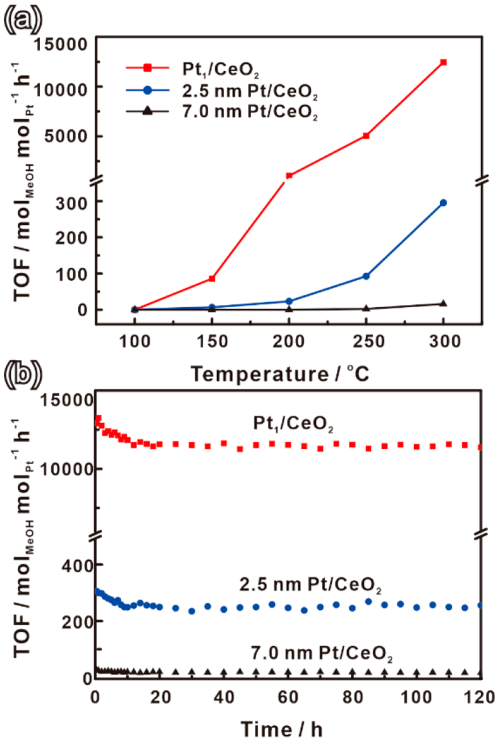

Figure 3. (a) Turnover frequency (TOF) of hydrogen production from methanol in terms of methanol conversion per Pt site of Pt_1/CeO_2, 2.5 nm Pt/CeO_2, and 7.0 nm Pt/CeO_2, at different temperatures. (b) Stability of Pt_1/CeO_2, 2.5 nm Pt/CeO_2, and 7.0 nm Pt/CeO_2 at 300 °C.

CeO_2 and almost 800 times that of 7.0 nm Pt/CeO_2. Furthermore, the single-site Pt_1/CeO_2 sample is highly stable: after reaction at 300 °C for 120 h, the catalyst keeps more than 90% of its best activity (Figure 3b). The decrease of activity at initial times is due to the loss of unstable absorb Pt sites on CeO_2 surface. The Pt content of Pt_1/CeO_2 catalyst decreased to 0.13% after the first 10 h of reaction and thereafter remains almost the same after 120 h reaction. After long-time reaction, there is still no Pt−Pt bond detected by EXAFS (Figure S6) indicating there is no agglomeration even after long-time reaction at 300 °C.

The dehydrogenation mechanism of methanol on the Pt surface has been experimentally examined using advanced techniques such as temperature programmed desorption (TPD), electron energy loss spectroscopy (EELS), infrared (IR), ultraviolet photoelectron spectroscopy (UPS), and Auger electron spectroscopy (AES). The dehydrogenation mechanism has also been examined via density functional theory (DFT) theoretical simulation.[10,23−25] These results indicate that, at low temperature, methanol molecularly absorbs at the surface of Pt and then decomposes to form methoxy species by breaking the O−H bond. Then successively, the three C−H bonds will be broken up and generate the final products CO_{ads} and H_{ads}. Importantly, both experimental and computational results demonstrated that smaller Pt nanoparticle size favors the methanol dehydrogenation due to the energy barriers of both O−H and C−H bond cleavage, much lower on the defects and steps of the Pt surface.

We also measured the catalytic hydrogen production performance of single-site Pt_1/CeO_2 catalyst as a function of the methanol feeding rate (Figure S7). At lower methanol feeding rate, the conversion of methanol is higher. When the feeding rate is 0.01 mL/min, methanol can totally convert to hydrogen, which proves that this catalyst can be applied in practical applications. As the feeding rate of methanol is increased, the TOF increases as well. The TOF is almost 15 000 h^{-1} at the feeding rate of 0.1 mL/min, illustrating the high catalytic activity of Pt_1/CeO_2 catalyst. We also synthesized a series of Pt_1/CeO_2 catalysts with different Pt content by controlling the feeding amount of Pt precursor (Figure S8a). All the Pt/CeO_2 catalysts performed high activity in methanol dehydrogenation; however, the TOFs of Pt/CeO_2-0.3% and -0.45% decrease due to Pt agglomeration at higher content (Figure S8b). No hydrogenation formation was detected with pure CeO_2 nanorods without Pt loading, indicating that the active site is Pt instead of CeO_2.

Single-site catalysts are typically systems where the activity of a central metal atom/atoms relies on interactions with heteroatomic ligands (such as N or O bridge) that anchor it to metal atoms of the substrate. The electronic structure and reactivity of Pt are very sensitive to support. In our study, the Pt element valence state was proven to be another factor influencing its catalytic activity. The Pt and Ce valence states of Pt_1/CeO_2, 2.5 nm Pt/CeO_2, and 7.0 nm Pt/CeO_2 are further confirmed by XPS analysis (Figure S9). Importantly, for the Pt 4f XPS spectra, the binding energies of Pt $4f_{2/7}$ and $4f_{2/5}$ in Pt_1/CeO_2 are close to Pt^{2+} species, indicating that the Pt single-site supported on CeO_2 is oxidized owing to the electron transfer of Pt to CeO_2.[26] Interestingly, the Pt species of 2.5 nm Pt/CeO_2 and 7.0 nm Pt/CeO_2 are mainly metallic Pt. The previous reports have certified that the Pt-CO bonding energy of CO absorption on positive Pt species is lower than on metallic Pt.[19,27] Thus, for the methanol dehydrogenation process, as the CO_{ads} species forms, it is much easier to desorb CO from positive Pt sites in Pt_1/CeO_2 than the metallic Pt sites of the other two catalysts (Figure S10). Therefore, the size effect and valence states of Pt may explain the relative catalytic activity of these catalyst samples, with activity ordered as single-site $Pt_1/CeO_2 \gg$ 2.5 nm $Pt/CeO_2 >$ 7.0 nm Pt/CeO_2.

The single-site Pt_1/CeO_2 also performed excellent catalytic activity in hydrogen production from other alcohols, namely, ethanol, 1-propanol, isopropanol, 1-buthanol, and benzyl alcohol (Figure 4). The proposed mechanism of the alcohol dehydrogenation process includes several steps. First, the alcohol molecules absorb on Pt sites and form $R_1R_2CHO_{ads}$ by breaking O−H bond, then dehydrogenation into $R_1R_2CO_{ads}$. As for methanol, after formaldehyde (CH_2O) intermediate is formed, it will further dehydrogenate to yield formyl (CHO) and carbon monoxide (CO).[10,24,25] Hence, compared to other alcohols, all the hydrogen in methanol can be released to generate two molecules of H_2 and leave CO behind. For other longer chain alcohols, after aldehydes or ketones formed, more energy is needed for additional dehydrogenation steps. Moreover, for primary alcohols, the activity of substrates is decreased with the growth of carbon chain, and after transformation to the corresponding aldehydes, some C−C bonds will be cleaved to form CO and alkanes. Besides, the hydrogen production from benzyl alcohol and isopropanol is higher, owing to that their first dehydrogenated products are more stable.

In summary, a well-defined single-site Pt_1/CeO_2 catalyst was developed, and its catalytic performance was evaluated for hydrogen generation from methanol. Importantly, compared to

DOI: 10.1021/jacs.9b09431
J. Am. Chem. Soc. 2019, 141, 17995−17999

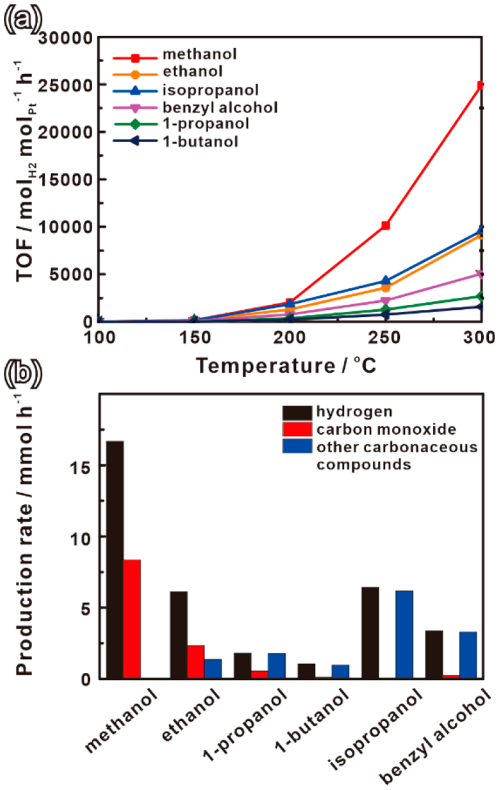

Figure 4. (a) Turnover frequency (TOF) of hydrogen production from different alcohol in terms of hydrogen production per Pt site of Pt_1/CeO_2 at different temperature. (b) Product diffusion of different alcohol at 300 °C by Pt_1/CeO_2 catalyst.

the Pt/CeO_2 nanoparticle catalysts (2.5 nm Pt/CeO_2 and 7.0 Pt/CeO_2), the single-site catalyst Pt_1/CeO_2 exhibited reaction rates that are 40 and 800 times higher, respectively. Moreover, beside the methanol, this single-site catalyst performed high efficiency in other liquid alcohol hydrogen production. Ultimately, this in-depth study highlights the benefits of a single-site catalyst and paves the way for further rational design of highly efficient catalysts for hydrogen production.

■ ASSOCIATED CONTENT

Supporting Information

The Supporting Information is available free of charge on the ACS Publications website at DOI: 10.1021/jacs.9b09431.

Experimental details, characterization data and partial catalytic data, including the synthesis of catalysts, the characterization of CeO_2 support and catalysts, the characterization of catalyst after reaction, and the catalytic result of some control tests (PDF)

■ AUTHOR INFORMATION

Corresponding Authors
*jisu@lbl.gov
*somorjai@berkeley.edu

ORCID
Lu-Ning Chen: 0000-0001-5434-4755
Yi-Sheng Liu: 0000-0002-1085-1947
Yi-Hsien Lu: 0000-0001-6572-5553
Vitalie Stavila: 0000-0003-0981-0432
Mark D. Allendorf: 0000-0001-5645-8246
Jinghua Guo: 0000-0002-8576-2172
Gabor A. Somorjai: 0000-0002-8478-2761

Notes
The authors declare no competing financial interest.

■ ACKNOWLEDGMENTS

This work was supported by the Hydrogen Materials Advanced Research Consortium (HyMARC), established as part of the Energy Materials Network by the U.S. Department of Energy, Office of Energy Efficiency and Renewable Energy, Fuel Cell Technologies Office, under Contract Number DE-AC02-05CH11231. This research used resources of the Advanced Light Source, which is a DOE Office of Science User Facility under contract no. DE-AC02-05CH11231. L.-N.C., Y.-S.L., J.G., D.P., and J.S. were supported by a User Project at The Molecular Foundry at Lawrence Berkeley National Laboratory, which is supported by the Office of Science of the U.S. Department of Energy under contract no. DE-AC02-05CH11231. Sandia National Laboratories is a multimission laboratory managed and operated by National Technology and Engineering Solutions of Sandia, LLC., a wholly owned subsidiary of Honeywell International, Inc., for the U.S. Department of Energy's National Nuclear Security Administration under Contract No. DE-NA-0003525. L.-N.C. and S.-B.W. thank the China Scholarship Council (CSC) for financial support.

■ REFERENCES

(1) Schultz, M. G.; Diehl, T.; Brasseur, G. P.; Zittel, W. Air Pollution and Climate-Forcing Impacts of a Global Hydrogen Economy. *Science* **2003**, *302*, 624.
(2) Steele, B. C. H.; Heinzel, A. Materials for fuel-cell technologies. *Nature* **2001**, *414*, 345.
(3) Schneemann, A.; White, J. L.; Kang, S. Y.; Jeong, S.; Wan, L. F.; Cho, E. S.; Heo, T. W.; Prendergast, D.; Urban, J. J.; Wood, B. C.; Allendorf, M. D.; Stavila, V. Nanostructured metal hydrides for hydrogen storage. *Chem. Rev.* **2018**, *118*, 10775.
(4) Allendorf, M. D.; Hulvey, Z.; Gennett, T.; Ahmed, A.; Autrey, T.; Camp, J.; Cho, E. S.; Furukawa, H.; Haranczyk, M.; Head-Gordon, M.; Jeong, S.; Karkamkar, A.; Liu, D.-J.; Long, J. R.; Meihaus, K. R.; Nayyar, I. H.; Nazarov, R.; Siegel, D. J.; Stavila, V.; Urban, J. J.; Veccham, S. P.; Wood, B. C. An assessment of strategies for the development of solid-state adsorbents for vehicular hydrogen storage. *Energy Environ. Sci.* **2018**, *11*, 2784.
(5) Preuster, P.; Papp, C.; Wasserscheid, P. Liquid organic hydrogen carriers (LOHCs): toward a hydrogen-free hydrogen economy. *Acc. Chem. Res.* **2017**, *50*, 74.
(6) Markiewicz, M.; Zhang, Y. Q.; Bö smann, A.; Brü ckner, N.; Thöming, J.; Wasserscheid, P.; Stolte, S. Environmental and health impact assessment of Liquid Organic Hydrogen Carrier (LOHC) systems—challenges and preliminary results. *Energy Environ. Sci.* **2015**, *8*, 1035.
(7) Teichmann, D.; Arlt, W.; Wasserscheid, P.; Freymann, R. A future energy supply based on Liquid Organic Hydrogen Carriers (LOHC). *Energy Environ. Sci.* **2011**, *4*, 2767.
(8) Palo, D. R.; Dagle, R. A.; Holladay, J. D. Methanol steam reforming for hydrogen production. *Chem. Rev.* **2007**, *107*, 3992.
(9) Liu, W.-C.; Baek, J.; Somorjai, G. A. The Methanol Economy: Methane and Carbon Dioxide Conversion. *Top. Catal.* **2018**, *61*, 530.
(10) Greeley, J.; Mavrikakis, M. Competitive paths for methanol decomposition on Pt (111). *J. Am. Chem. Soc.* **2004**, *126*, 3910.
(11) Kuhn, J. N.; Huang, W.; Tsung, C.-K.; Zhang, Y.; Somorjai, G. A. Structure Sensitivity of Carbon–Nitrogen Ring Opening: Impact of Platinum Particle Size from below 1 to 5 nm upon Pyrrole Hydrogenation Product Selectivity over Monodisperse Platinum

Nanoparticles Loaded onto Mesoporous Silica. *J. Am. Chem. Soc.* **2008**, *130*, 14026.

(12) Tsung, C. K.; Kuhn, J. N.; Huang, W. Y.; Aliaga, C.; Hung, L. I.; Somorjai, G. A.; Yang, P. D. Sub-10 nm platinum nanocrystals with size and shape control: catalytic study for ethylene and pyrrole hydrogenation. *J. Am. Chem. Soc.* **2009**, *131*, 5816.

(13) Qiao, B.; Wang, A.; Yang, X.; Allard, L. F.; Jiang, Z.; Cui, Y.; Liu, J.; Li, J.; Zhang, T. Single-atom catalysis of CO oxidation using Pt1/FeOx. *Nat. Chem.* **2011**, *3*, 634.

(14) Lin, L.; Zhou, W.; Gao, R.; Yao, S.; Zhang, X.; Xu, W.; Zheng, S.; Jiang, Z.; Yu, Q.; Li, Y. W.; Shi, C.; Wen, X. D.; Ma, D. Low-temperature hydrogen production from water and methanol using Pt/α-MoC catalysts. *Nature* **2017**, *544*, 80.

(15) Liu, P.; Zhao, Y.; Qin, R.; Mo, S.; Chen, G.; Gu, L.; Chevrier, D. M.; Zhang, P.; Guo, Q.; Zang, D.; Wu, B.; Fu, G.; Zheng, N. Photochemical route for synthesizing atomically dispersed palladium catalysts. *Science* **2016**, *352*, 797.

(16) Yang, X. F.; Wang, A. Q.; Qiao, B. T.; Li, J.; Liu, J. Y.; Zhang, T. Single-atom catalysts: a new frontier in heterogeneous catalysis. *Acc. Chem. Res.* **2013**, *46*, 1740.

(17) Chen, Y.; Ji, S.; Chen, C.; Peng, Q.; Wang, D.; Li, Y. Single-atom catalysts: synthetic strategies and electrochemical applications. *Joule* **2018**, *2*, 1242.

(18) Nie, L.; Mei, D.; Xiong, H.; Peng, B.; Ren, Z.; Hernandez, X.; DeLaRiva, A.; Wang, M.; Engelhard, M. H.; Kovarik, L.; Datye, A. K.; Wang, Y. Activation of surface lattice oxygen in single-atom Pt/CeO2 for low-temperature CO oxidation. *Science* **2017**, *358*, 1419.

(19) Chen, J.; Wanyan, Y.; Zeng, J.; Fang, H.; Li, Z.; Dong, Y.; Qin, R.; Wu, C.; Liu, D.; Wang, M.; Kuang, Q.; Xie, Z.; Zheng, L. Surface Engineering Protocol To Obtain an Atomically Dispersed Pt/CeO2 Catalyst with High Activity and Stability for CO Oxidation. *ACS Sustainable Chem. Eng.* **2018**, *6*, 14054.

(20) Rioux, R. M.; Song, H.; Hoefelmeyer, J. D.; Yang, P.; Somorjai, G. A. High-surface-area catalyst design: synthesis, characterization, and reaction studies of platinum nanoparticles in mesoporous SBA-15 silica. *J. Phys. Chem. B* **2005**, *109*, 2192.

(21) Aliaga, C.; Park, J. Y.; Yamada, Y.; Lee, H. S.; Tsung, C. K.; Yang, P. D.; Somorjai, G. A. Sum frequency generation and catalytic reaction studies of the removal of organic capping agents from Pt nanoparticles by UV− ozone treatment. *J. Phys. Chem. C* **2009**, *113*, 6150.

(22) Kappers, M. J.; van der Maas, J. H. Correlation between CO frequency and Pt coordination number. A DRIFT study on supported Pt catalysts. *Catal. Lett.* **1991**, *10*, 365.

(23) Gibson, K. D.; Dubois, L. H. Step effects in the thermal decomposition of methanol on Pt (111). *Surf. Sci.* **1990**, *233*, 59.

(24) Greeley, J.; Mavrikakis, M. A first-principles study of methanol decomposition on Pt (111). *J. Am. Chem. Soc.* **2002**, *124*, 7193.

(25) Desai, S. K.; Neurock, M.; Kourtakis, K. A periodic density functional theory study of the dehydrogenation of methanol over Pt (111). *J. Phys. Chem. B* **2002**, *106*, 2559.

(26) Wiebenga, M. H.; Kim, C. H.; Schmieg, S. J.; Oh, S. H.; Brown, D. B.; Kim, D. H.; Lee, J. H.; Peden, C. H. F. Deactivation mechanisms of Pt/Pd-based diesel oxidation catalysts. *Catal. Today* **2012**, *184*, 197.

(27) Mao, M.; Lv, H.; Li, Y.; Yang, Y.; Zeng, M.; Li, N.; Zhao, X. Metal Support Interaction in Pt Nanoparticles Partially Confined in the Mesopores of Microsized Mesoporous CeO2 for Highly Efficient Purification of Volatile Organic Compounds. *ACS Catal.* **2016**, *6*, 418.

DOI: 10.1021/jacs.9b09431
J. Am. Chem. Soc. 2019, 141, 17995−17999